NASA Technical Memorandum 107270
AIAA–96–2584

Validation of High Aspect Ratio Cooling in a 89 kN (20,000 lb_f) Thrust Combustion Chamber

Mary F. Wadel and Michael L. Meyer
Lewis Research Center
Cleveland, Ohio

Prepared for the
32nd Joint Propulsion Conference
cosponsored by AIAA, ASME, SAE, and ASEE
Lake Buena Vista, Florida, July 1–3, 1996

National Aeronautics and
Space Administration

Validation of High Aspect Ratio Cooling in a 89 kN (20,000 lb_f) Thrust Combustion Chamber

Mary F. Wadel†
and
Michael L. Meyer†

National Aeronautics and Space Administration
Lewis Research Center
Cleveland, Ohio 44135

Abstract

In order to validate the benefits of high aspect ratio cooling channels in a large scale rocket combustion chamber, a high pressure, 89 kN (20,000 lb_f) thrust, contoured combustion chamber was tested in the NASA Lewis Research Center Rocket Engine Test Facility. The combustion chamber was tested at chamber pressures from 5.5 to 11.0 MPa (800-1600 psia). The propellants were gaseous hydrogen and liquid oxygen at a nominal mixture ratio of six, and liquid hydrogen was used as the coolant. The combustion chamber was extensively instrumented with 30 backside skin thermocouples, 9 coolant channel rib thermocouples, and 10 coolant channel pressure taps. A total of 29 thermal cycles, each with one second of steady state combustion, were completed on the chamber. For 25 thermal cycles, the coolant mass flow rate was equal to the fuel mass flow rate. During the remaining four thermal cycles, the coolant mass flow rate was progressively reduced by 5, 6, 11, and 20 percent. Computer analysis agreed with coolant channel rib thermocouples within an average of 9 percent and with coolant channel pressure drops within an average of 20 percent. Hot-gas-side wall temperatures of the chamber showed up to a 25 percent reduction, in the throat region, over that of a conventionally cooled combustion chamber. Reducing coolant mass flow yielded a reduction of up to 27 percent of the coolant pressure drop from that of a full flow case, while still maintaining up to a 13 percent reduction in hot-gas-side wall temperature from that of a conventionally cooled combustion chamber.

† - Member, AIAA.

Introduction

The design of a high pressure, regeneratively cooled, liquid rocket engine thrust chamber liner evolves from a compromise between the goal of minimizing hot-gas-side wall temperatures and minimizing the coolant jacket pressure drop. The hot-gas-side wall temperature is life limiting for the combustion chamber, but reducing it typically requires increasing coolant velocity, either by reducing the flow area or increasing coolant flow. Both of these options increase the coolant pressure drop, which in turn imposes greater performance requirements from the turbomachinery.

One method of reducing the hot-gas-side wall temperature, while at the same time minimizing pressure drop, is the use of high-aspect-ratio cooling channels (HARCC) (typically > 4). HARCC provide the opportunity to increase cooling channel surface area or to increase both the cooling channel surface area and the number of cooling channels over that for a conventional design. By increasing the cooling channel surface area, heat from the hot-gas-side wall is more efficiently transferred to the coolant. The increased height and number of the ribs between the HARCC also enhance the heat transfer from the chamber liner to the coolant (i.e. enhanced 'fin' effect). In addition, it is possible to fabricate HARCC with sufficiently greater total flow area to reduce pressure drop over a conventional design, and still gain an increase in the heat transfer capability.

Previous experimental tests compared the cooling capabilities of conventional cooling channels to that of HARCC.[1] These tests were performed on straight cooling passages at a modest chamber pressure (4.14 MPa (600 psia)). The results showed that with a HARCC chamber, a significant reduction in hot-gas-side wall temperature (28 percent) could be achieved for the same pressure drop, or, alternatively, the coolant pressure drop could be further reduced by lowering the coolant mass flow while still achieving a reduction in

the hot-gas-side wall temperature.

Conventional combustion chamber designs using low-aspect-ratio (typically < 4) cooling channels rely on the curvature enhancement factor in the throat region to reduce the hot-gas-side wall temperature. The increased heat transfer is due to secondary flow in the coolant as it traverses the curved passages in the throat. A concern with a chamber design using HARCC is whether the tall, narrow cooling channels diminish the secondary flow effects and in turn reduce the curvature enhancement factor. Due to the concerns with curvature and the lower chamber pressure of the previous experimental tests, testing with a high pressure, contoured chamber was deemed necessary.

In order to provide answers to these issues, validate the merits of the HARCC concept, and provide a database for future rocket engine designs, an extensively instrumented, high pressure, contoured, HARCC chamber was tested in the NASA Lewis Research Center Rocket Engine Test Facility (RETF). This paper discusses the experimental results of the HARCC chamber testing and presents comparisons of the experimental results with two analysis methods.

Rocket Engine Test Hardware

For the test program, three rocket engine combustion chambers were run. Two chambers were copper heat sink chambers. These chambers were used to tune the propellant control valves for the test matrix flow rates in order to prevent unnecessary damage to the critical test hardware. The third chamber was actively cooled and used HARCC.

Injector

A full flow injector designed for use with liquid oxygen (LOX) and gaseous hydrogen (GH_2) was used for the test program. The LOX was injected through 91 tubes arranged in concentric circles. The GH_2 was injected through a porous-sintered-wire mesh face plate. Two pressure taps, placed 180 degrees apart, were located on the faceplate between the outer and next inner row of LOX tubes. The injector, after being fired, can be seen in figure 1.

Heat Sink Chambers

The two copper heat sink chambers were made from oxygen-free, high-conductivity (OFHC) copper. They had a combustion chamber diameter of 12.2 cm (4.8 inches) and a throat diameter of 6.6 cm (2.6 inches) with a continuous curve contour. The exit nozzle was a 15 degree conical nozzle, and the total combustion chamber length was 26 cm (10.25 inches). The chamber was ignited with a spark torch igniter through a port on the side of the chamber. Figure 1 shows the nozzle end of the two heat sink chambers and the injector manifolding, after testing.

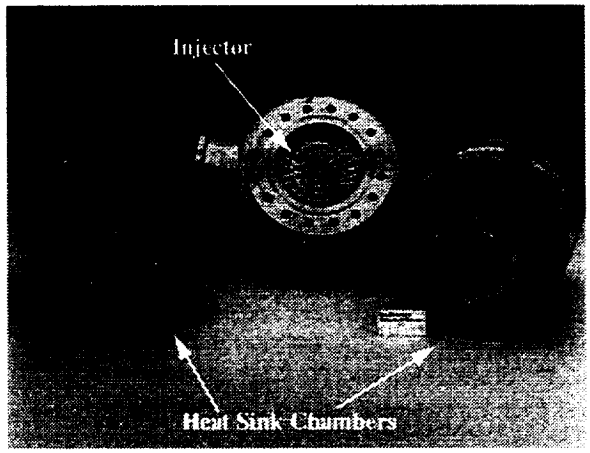

Figure 1. - Copper heat sink chambers and injector. Copper heat sink chambers viewed from nozzle exit.

HARCC Chamber

The single HARCC chamber was made with an OFHC copper inner liner and an electroformed nickel structural jacket. It had a combustion chamber diameter of 12.2 cm (4.8 inches) and a throat diameter of 6.6 cm (2.6 inches) with a continuous curve contour. The nozzle was bell-shaped with an exit angle of 36 degrees and was truncated at an expansion area ratio of 7.5. The total combustion chamber length was 33.7 cm (13.25 inches). A picture of the HARCC chamber, fully instrumented, is provided in figure 2, and a plot of the contour along with analysis points is presented in figure 3.

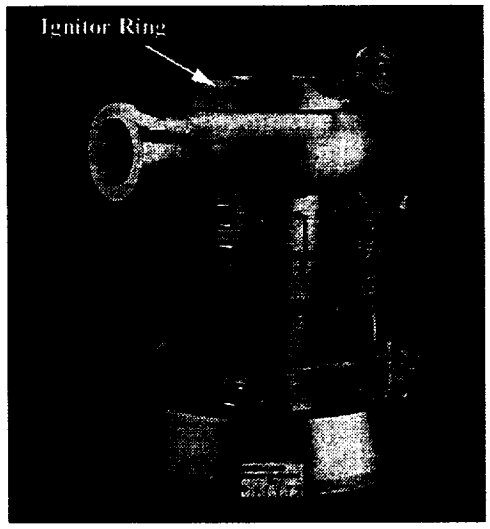

Figure 2. - HARCC chamber prior to testing.

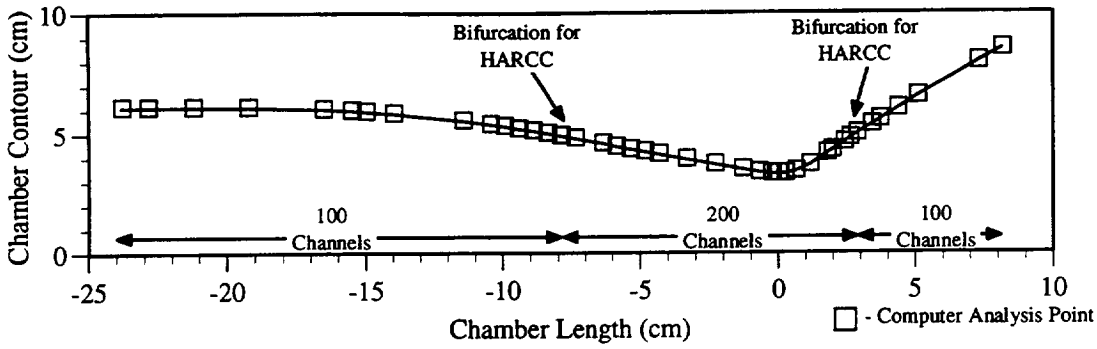

Figure 3. - Combustion chamber contour with bifurcation and computer analysis points indicated.

The HARCC chamber was designed to be cooled in counter flow with liquid hydrogen (LH_2).[2] The OFHC copper liner was milled with 100 conventional coolant channels. These channels had a nominal aspect ratio of 2.5. In the critical heat flux area the cooling channels were bifurcated into 200 channels and the aspect ratio was increased to a range of five to eight. The location of the various cooling channel regions are shown along the contour in figure 3 with a picture of the milled liner shown in figure 4.

Ignition using the HARCC chamber was accomplished with a spark torch igniter attached to a spacer ring that was placed between the injector manifold system and the combustion chamber. The spacer ring was used because the existing injector did not lend itself to modification and the integrity of the cooling jacket needed to be retained for these experiments. A picture of the igniter ring installed on the HARCC chamber is shown in figure 2.

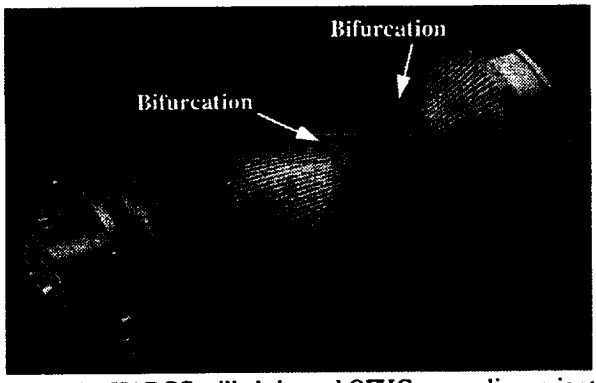

Figure 4. - HARCC milled channel OFHC copper liner prior to electroforming.

Instrumentation

In order to obtain critical heat transfer data to validate the HARCC concept, the HARCC chamber was extensively instrumented. Nine thermocouples were inserted into holes drilled in the center of the coolant channel ribs in the nozzle and combustion chamber sides of the bifurcated regions. The thermocouples were spring loaded against the bottom of the rib holes. A cross-sectional drawing of an ideal rib thermocouple placement is given in figure 5. A set of rib

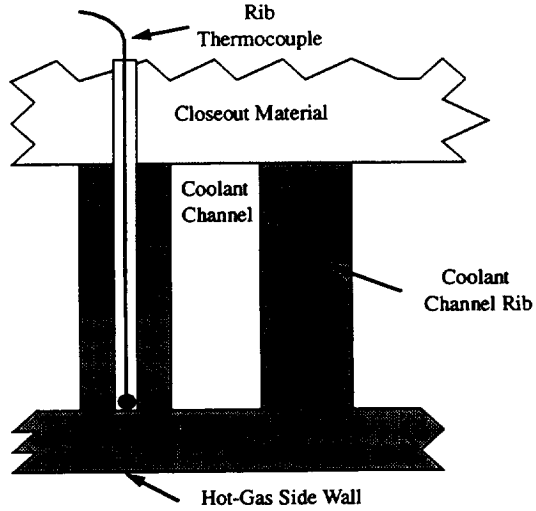

Figure 5. - Ideal rib thermocouple placement.

thermocouples was placed at one axial location on the nozzle side of the bifurcation region and two sets of rib thermocouples were placed at two axial locations on the combustion chamber side of the bifurcation region. At each axial location, there were two to four thermocouples placed 90 to 180 degrees apart. Figure 6 shows the axial locations used for the rib thermocouples. Due to the limited thickness of the channel ribs, no rib thermocouples could be placed in the bifurcated channel region.

The HARCC chamber was also instrumented with 30 backside skin thermocouples placed along the entire chamber length. Twelve of the backside thermocouples were placed at the same axial locations as the rib thermocouples. Each location had four backside skin thermocouples placed 90 degrees apart. The remaining backside skin thermocouples were placed at several axial locations within the bifurcation region. Each axial location had four backside skin

thermocouples placed 90 degrees apart with the exception of one location, which had two backside skin thermocouples placed 180 degrees apart. Figure 6 shows the axial locations of the backside skin thermocouples.

The HARCC chamber was also instrumented with ten coolant pressure taps, placed in three axial locations along the combustion chamber. The pressure taps were placed in the same axial locations as the rib thermocouples, as shown in figure 6. At each of the axial locations there were two to four pressure taps placed 90 degrees apart.

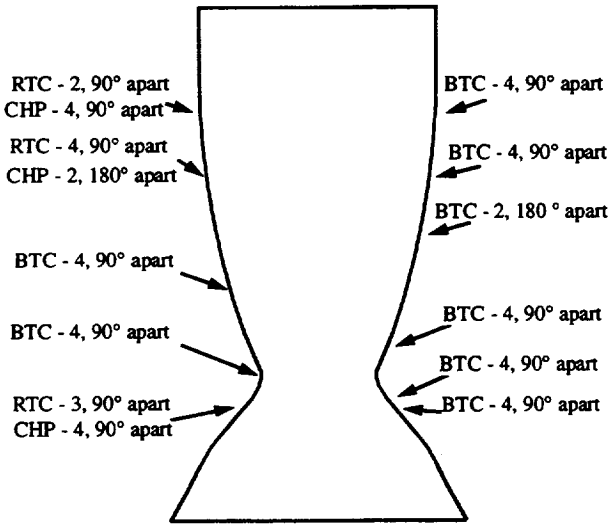

RTC - Rib Thermocouple
CHP - Coolant Channel Pressure Tap
BTC - Backside Skin Thermocouple

Figure 6. - Combustion chamber contour with rib thermocouple, backside skin thermocouple, and coolant channel pressure tap locations, quantity, and placement indicated.

Test Procedure

The testing was conducted on Stand A at RETF, a sea level rocket engine test stand. RETF uses pressurized tanks to supply propellants and coolant to the combustion chamber. The LOX and GH_2 were supplied to the injector manifolds and LH_2 was supplied to the cooling inlet manifold at the exit plane of the nozzle. The LOX and GH_2 were combusted in the combustion chamber and the LH_2 was exhausted to a burnoff stack.

Each individual firing of a chamber was considered a thermal cycle. The heat sink cycles consisted only of a combustion portion. The total combustion time was limited to reduce damage to the heat sink chamber with only enough steady-state combustion time allocated to obtain relevant flow rate information required for proper valve tuning. Even at these short cycle times, the heat sink chambers experienced significant damage after several cycles (see figure 1). The two chambers did, however, provide sufficient run time to tune the facility valves.

For the HARCC chamber, a thermal cycle consisted of a chilldown portion prior to ignition and a combustion portion. The chilldown portion was used to bring the chamber wall to LH_2 temperatures. The combustion portion was made long enough to provide at least one second of steady-state combustion. One second of steady-state combustion was sufficient for the rib thermocouples to reach steady-state. Table 1 provides a breakdown of the cycle times for each type of chamber.

Table 1. - Thermal cycle timing for each chamber type.

	Heat Sink Chamber	HARCC Chamber
LH_2 Chilldown Time	N/A	2 sec
Total Combustion Time	2.5 sec	3.5 sec
Steady-State Combustion Time	0.2 sec	1 sec
Total Cycle Time	2.5 sec	5.5 sec

For this test program, many precautions were taken to reduce the risk of failure of the HARCC chamber not attributable to the cooling channels. The largest of these precautions was to use the heat sink chambers to tune the propellant control valves. The second of these precautions was to step the chamber pressure up in 1.4 MPa to 2.8 MPa (200 to 400 psia) increments until the highest chamber pressure goal of 11 MPa (1600 psia) was reached. Table 2 presents the test parameters at each of these test conditions. The third of these precautions was to set the coolant inlet pressure high enough to keep the coolant channel pressure along the entire length of the chamber above the desired chamber pressure in case a crack should form in the

Table 2. - Test Parameters.

Chamber Pressure MPa (psia)	5.5 (800)	8.3 (1200)	9.7 (1400)	11 (1600)
Mixture Ratio	6	6	6	6
LOX Mass Flow kg/sec (lb_m/sec)	6.9 (15.3)	10.3 (22.8)	12.1 (26.6)	13.8 (30.4)
GH_2 Mass Flow kg/sec (lbm/sec)	1.2 (2.6)	1.7 (3.8)	2.0 (4.4)	2.3 (5.1)
LH_2 Mass Flow kg/sec (lb_m/sec)	1.2 (2.6)	1.7 (3.8)	2.0 (4.4)	≤2.3 (≤5.1)
Number of Thermal Cycles	6	10	3	10

chamber wall. Finally, the last of these precautions was to use the final thermal cycles to investigate the effects of coolant mass flow on the coolant pressure drop and hot-gas-side wall temperature by progressively reducing the coolant channel mass flow rate. The risk of over heating the hot-gas-side wall was greatest during these reduced coolant flow tests.

Analysis

Two analysis methods were used to analyze the steady-state experimental data. The first method involved using a three dimensional rocket thermal evaluation code (RTE) independently.[3] This code requires user input of a correlation coefficient (Cg) for the hot-gas side. For this study, the Cg coefficient profile for the combustion chamber was based on previous experience with similar, although not identical, chambers. The second method involved using an iteration of heat transfer rate and hot-gas-side wall temperature between RTE and a nozzle analysis code, TDK, which uses an inviscid, boundary layer analysis technique.[4] For both methods, a rocket combustion analysis code (ROCCID) was used to obtain an axial profile of the mixture ratio in the chamber upstream of the throat.[5]

The two analysis methods were used to predict rib thermocouple and coolant channel pressure data that could be compared to the experimental data. They were also used to obtain hot-gas-side wall predictions for the entire chamber profile. Along with the analysis of the HARCC data, the analysis methods were also used to analyze a comparable baseline engine design using a conventional cooling design of 100 cooling channels at a continuous 2.5 aspect ratio.[2]

Results and Discussion

The heat sink and HARCC chambers were successfully tested at RETF. Figure 7 shows the HARCC chamber on the test stand during test firing. After the flow rates were properly set with the heat sink chambers, the HARCC chamber was tested for 29 complete thermal cycles. Four of the thermal cycles were run at the nominal chamber pressure of 11MPa (1600 psia) with progressively lower coolant mass flow rates. The HARCC chamber suffered no serious damage during testing.

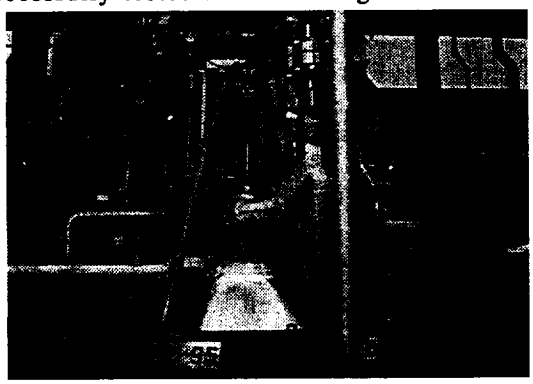

Figure 7. - HARCC combustion chamber on test stand during test firing.

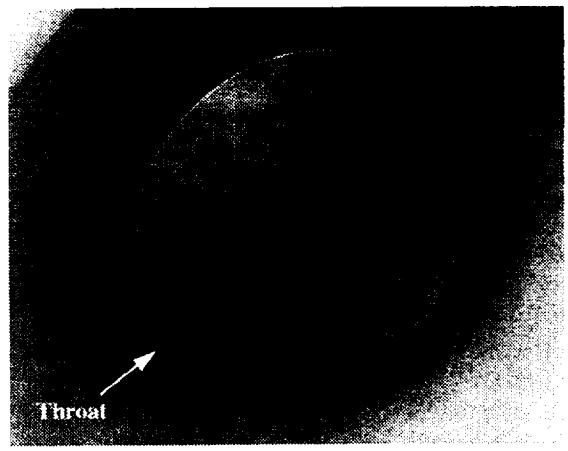

Figure 8. - Close up of HARCC combustion chamber throat, viewed from the nozzle exit, with no visible damage after 29 thermal cycles.

Visual examination of the HARCC chamber after testing revealed no deterioration of the throat and minimal roughening of the combustion chamber wall in the bifurcation region. Figure 8 is a close-up picture of the HARCC chamber throat viewed from the nozzle exit. No roughening was observed in the throat region. Figure 9 is a close up of the HARCC combustion chamber viewed from the injector end. The streamwise discolorations are indicative of injector mixture ratio discontinuities (excess oxygen) along the wall, but caused no damage to the liner surface. Some roughening of the chamber wall can be seen at the point where the coolant channels were bifurcated.

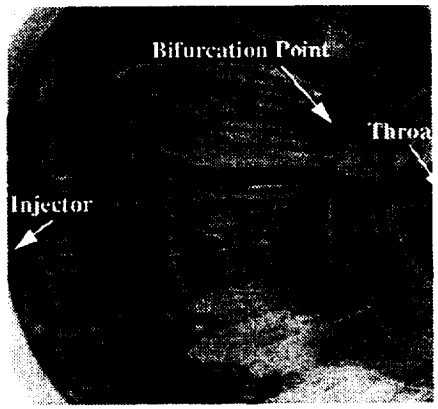

Figure 9. - Close up of HARCC combustion chamber, viewed from the injector end, showing minimal wall roughening at point of bifurcation.

Results from the 30 backside skin thermocouples revealed no backside wall temperature anomalies. During the combustion portion of the HARCC chamber thermal cycle, the backside skin thermocouples did not have enough time to reach a steady-state. Therefore, comparison of the backside skin thermocouples with a steady-state code analysis was not possible. However, because less than one percent of the total hot-gas-side heat flux was being conducted into the structural jacket, the heat sink effects of the nickel jacket had an insignificant effect on the reported results.

Comparison With Analysis

Typical test readings, which most closely matched the test parameters that were presented in table 2, were analyzed using the two analysis methods. This involved using the specific chamber pressure, flow rates, and inlet temperatures for the individual reading as input into the codes. Table 3 presents the chamber pressure, mixture ratio, and LH_2 coolant flow rate from each of the test readings.

Both the RTE/Cg and RTE/TDK methods produce output which gives the predicted cross-sectional temperature profile of the coolant channel, coolant channel rib, closeout material, and hot-gas-side wall at a given axial location. It also provides the predicted coolant channel pressure for the given axial location. From the predictions for each of the readings shown in table 3, the experimental rib thermocouple temperatures and coolant channel pressure drops were compared. Also, the resulting hot-gas-side wall temperatures from these readings were investigated.

Table 3. - Conditions for typical test readings.

Test Reading	53	68	73	86
Chamber Pressure MPa (psia)	5.6 (818)	8.1 (1167)	9.9 (1435)	10.9 (1586)
Mixture Ratio	6.2	5.9	5.9	5.7
LH_2 Coolant Flow Rate kg/sec (lb_m/sec)	1.2 (2.6)	1.7 (3.8)	2.0 (4.4)	2.3 (5.1)

Rib Thermocouple Comparison

The rib thermocouple temperatures from the test data and analysis were compared. After machining, the rib depth of the nine rib thermocouples were slightly different from the ideal placement shown in figure 5. These different depths were taken into consideration for the analysis. Figures 10 through 13 show the results for each chamber pressure tested along with the predictions for each rib thermocouple. As can be seen in all four of the figures, the RTE/TDK method predicted the rib thermocouple temperatures well. The average RTE/TDK prediction varied from the test results by 9 percent, with the maximum difference being 19 percent and the minimum difference being 1 percent. However, using RTE/Cg provided an extremely conservative prediction. The average RTE/Cg prediction varied from the test data by 40 percent, with the maximum difference being 84 percent and the minimum difference being 0 percent. Although RTE/Cg did not predict the

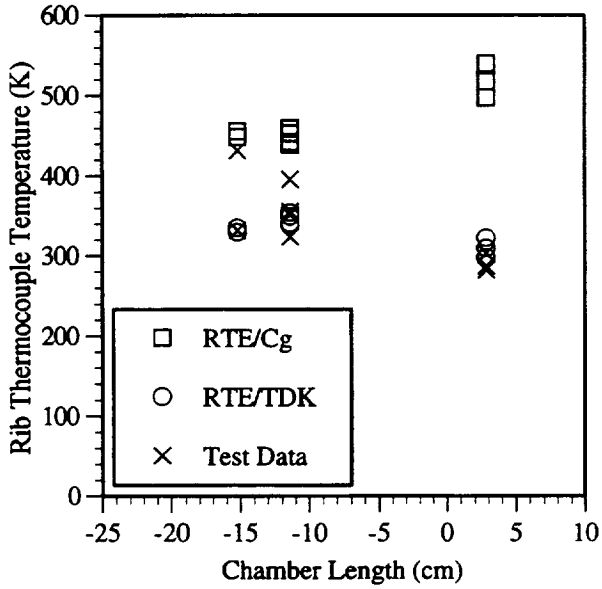

Figure 10. - Rib thermocouple temperature comparison of experimental versus predicted values for a nominal chamber pressure of 5.5 MPa (800 psia) (using Rdg. 53).

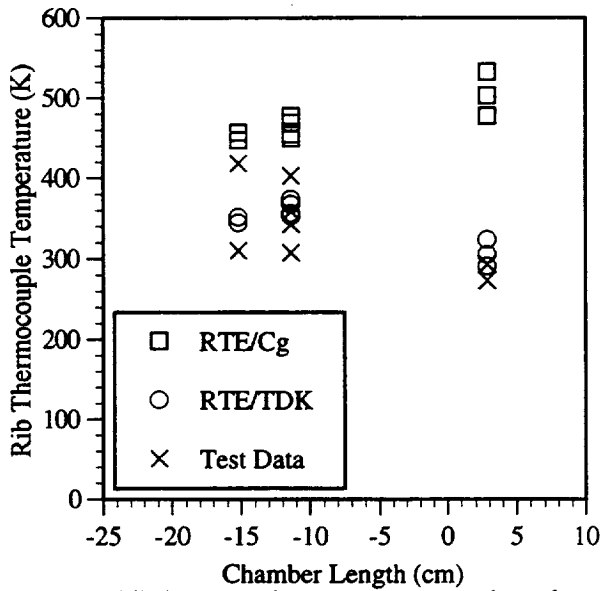

Figure 11. - Rib thermocouple temperature comparison of experimental versus predicted values for a nominal chamber pressure of 8.3 MPa (1200 psia) (using Rdg. 68).

rib thermocouple data well, improvement of the Cg profile used, by testing a calorimeter with this specific chamber contour, would allow RTE/Cg to predict better. However, from the results obtained here, it can be determined that the RTE/TDK method of prediction is superior to using RTE/Cg when predicting combustion chamber wall temperatures, without the additional testing of a calorimeter chamber.

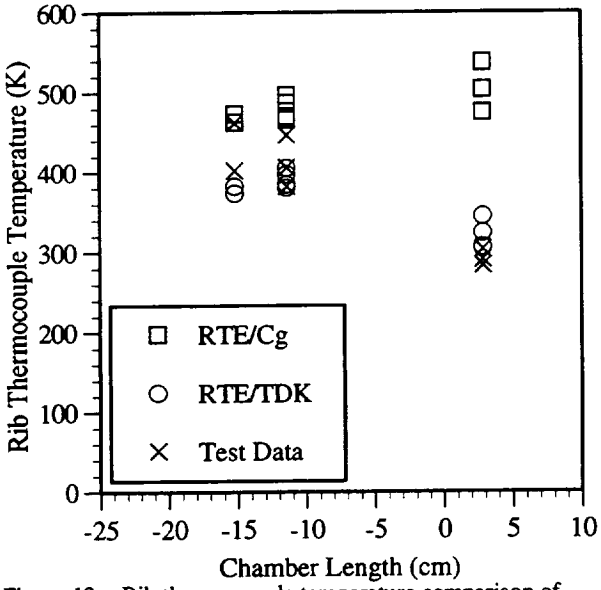

Figure 12. - Rib thermocouple temperature comparison of experimental versus predicted values for a nominal chamber pressure of 9.7 MPa (1400 psia) (using Rdg.73).

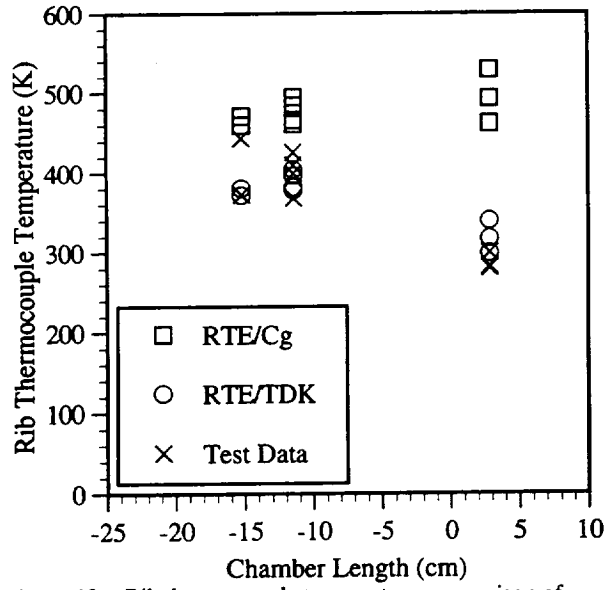

Figure 13. - Rib thermocouple temperature comparison of experimental versus predicted values for a nominal chamber pressure of 11 MPa (1600 psia) (using Rdg 86).

Coolant Channel Pressure Drop Comparison

The coolant channel pressure drops from the test data and analysis were compared. The coolant channel inlet pressure is an input into the codes used for the analysis. Therefore, the specific coolant inlet pressures for each test case were used for the analysis comparisons. Figures 14 through 17 show the results for each chamber pressure tested along with the predictions for each channel pressure measured. As can be seen in all four of the figures, both analysis methods

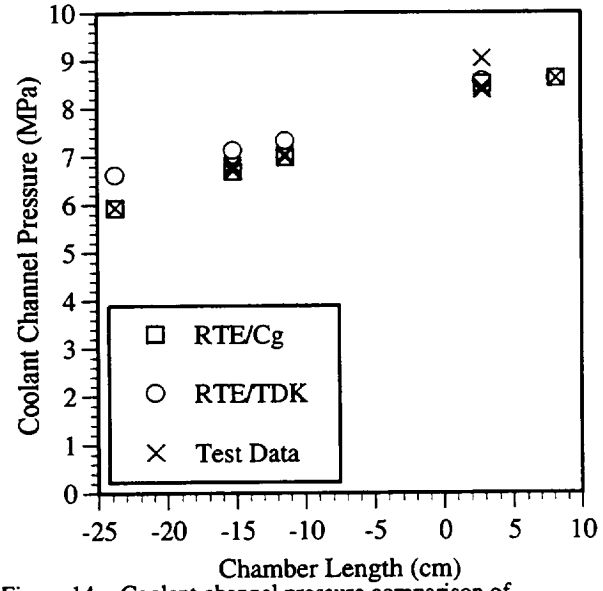

Figure 14. - Coolant channel pressure comparison of experimental versus predicted values for a nominal chamber pressure of 5.5 MPa (800 psia) (using Rdg. 53).

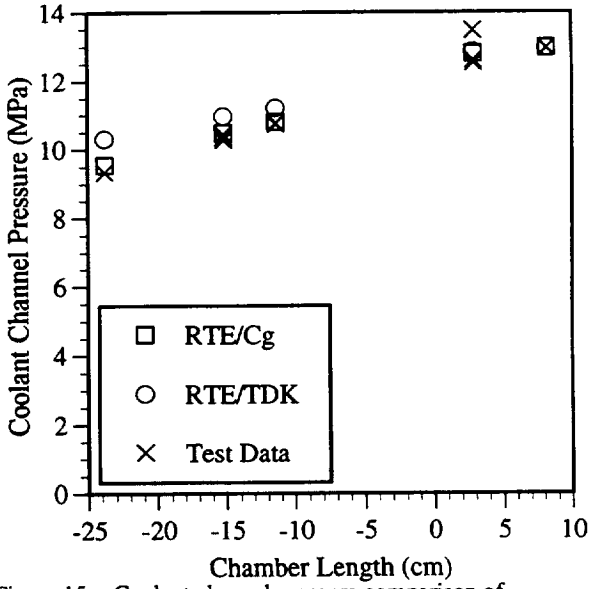

Figure 15. - Coolant channel pressure comparison of experimental versus predicted values for a nominal chamber pressure of 8.3 MPa (1200 psia) (using Rdg. 68).

were able to favorably predict the coolant channel pressures and coolant channel pressure drops given by the test results. The average RTE/TDK prediction of coolant pressure drop varied from the test results by 25 percent, with the maximum difference being 30 percent and the minimum difference being 20 percent. The average RTE/Cg prediction of coolant pressure drop varied from the test results by 10 percent, with the maximum difference being 16 percent and the minimum difference being 4 percent. These percentages are based upon the coolant pressure drop up to the channel pressure tap closest to the injector, which was located 15.3 cm (6 inches) upstream of the throat. They do not include the pressure drop between this coolant pressure tap and the test data exit pressures and predicted coolant exit pressures. These were omitted because the coolant exit pressure was measured downstream of a fitting and not directly in the coolant exit manifolding, whereas the analysis methods predicted an exit pressure that would reflect a pressure taken directly in the exit manifold. Although the RTE/Cg method appears to predict the coolant pressure drop better than the RTE/TDK method, the difference is due solely to the overprediction of heat flux into the coolant by the RTE/Cg method, as evidenced by the overprediction of the rib thermocouple temperatures (see figures 10 - 13).

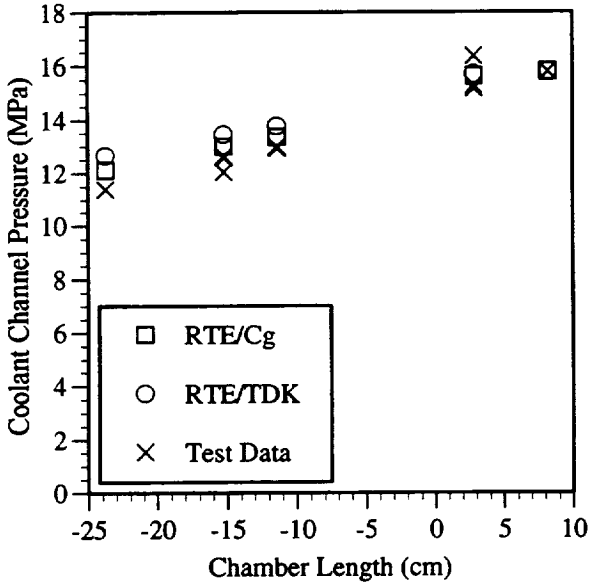

Figure 16. - Coolant channel pressure comparison of experimental versus predicted values for a nominal chamber pressure of 9.7 MPa (1400 psia) (using Rdg. 73).

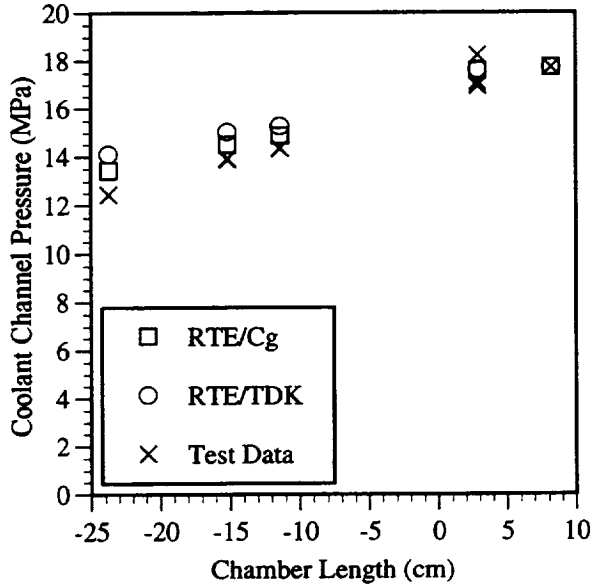

Figure 17. - Coolant channel pressure comparison of experimental versus predicted values for a nominal chamber pressure of 11 MPa (1600 psia) (using Rdg. 86).

Hot-Gas-Side Wall Temperature Comparison

The predicted hot-gas-side wall temperatures for each test reading given in table 3 for the HARCC chamber were compared to predictions of a baseline chamber using conventional aspect ratio coolant channels at that chamber pressure. Figures 18 through 21 show the HARCC and baseline hot-gas-side wall temperature predictions for each of the chamber pressures selected. All four figures show that using HARCC in the critical heat-flux area dramatically reduces the hot-gas-side wall temperature from that of a conventionally cooled chamber. Using the throat temperature as a reference, HARCC can reduce the hot-gas-side wall temperature by as much as 25 percent. This compares with the previous straight-channel,

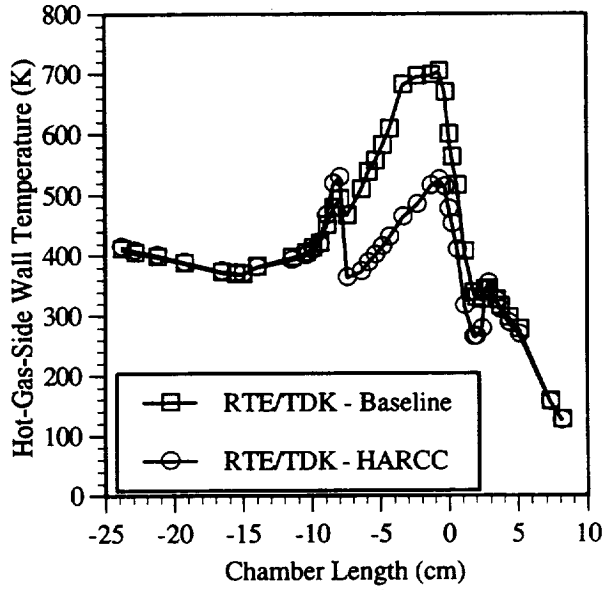

Figure 18. - Predicted hot-gas-side wall temperature comparisons for a nominal chamber pressure of 5.5 MPa (800 psia) (using Rdg. 53).

subscale testing, which showed a reduction of 28 percent. The additional temperature spikes, beyond that of the throat region, seen in the HARCC temperature profiles can be attributed to the bifurcation of the channels. With current milling techniques, bifurcation points result in an exaggerated flow area increase, which reduces the heat transfer capabilities at that point. The result can be a local increase in the hot-gas-side wall temperature which can cause damage to the chamber liner, such as roughening or even coolant channel cracks. These can be avoided by bifurcating the channels further away from the critical heat flux area, where the hot-gas-side wall temperature is lower. The roughening of the combustion chamber wall at the point of bifurcation of the HARCC chamber, shown in figure 8, can be attributed to this phenomena.

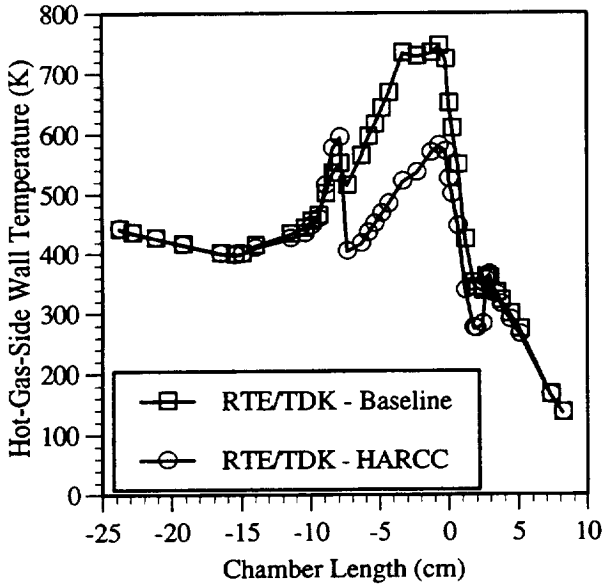

Figure 19. - Predicted hot-gas-side wall temperatures for a nominal chamber pressure of 8.3 MPa (1200 psia) (using Rdg. 68).

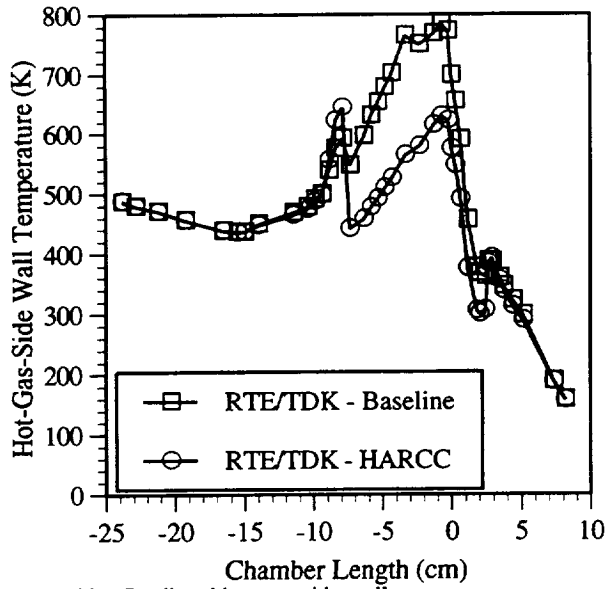

Figure 20. - Predicted hot-gas-side wall temperature comparisons for a nominal chamber pressure of 9.7 MPa (1400 psia) (using Rdg. 73).

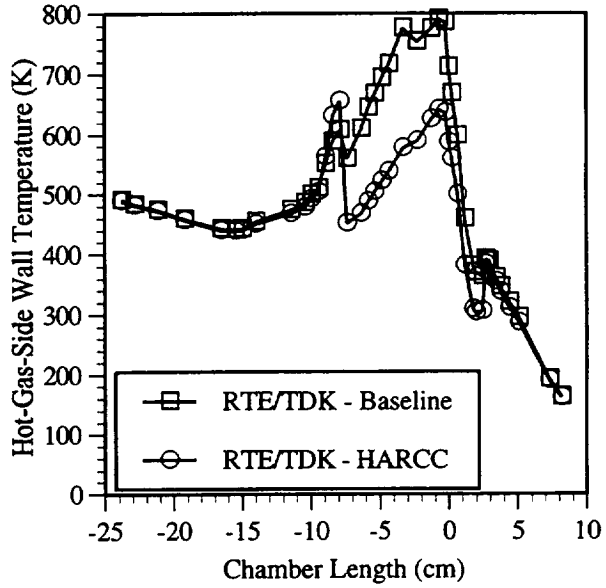

Figure 21. - Predicted hot-gas-side wall temperatures for a nominal chamber pressure of 11 MPa (1600 psia) (using Rdg. 86).

Effects of Reduced Coolant Mass Flow

The effects of reduced coolant mass flow on coolant channel pressure drop and hot-gas-side wall temperature were investigated. The final four thermal cycles of the HARCC chamber progressively reduced the coolant mass flow by 5, 6, 11, and 20 percent while maintaining a nominal chamber pressure of 11 MPa (1600 psia). Figure 22 shows the coolant pressure drop, for each of the reduced mass flow cases, measured during testing, plotted along with the hot-gas-side wall temperature predicted for the throat region. The predicted coolant pressure drop and throat hot-gas-side wall temperature for a comparable conventionally cooled chamber is provided for reference. As can be seen in figure 22, reducing coolant mass flow by as much as 20 percent, lowers the coolant pressure drop by as much as 27 percent, while still retaining a reduction in hot-gas-side wall temperature at the throat of 13 percent from that of a conventionally cooled chamber. The trend of the data in figure 22 follows the same trends as that of the previous subscale testing. Therefore, the potential for further coolant mass flow reduction was extrapolated from the test data (shown in figure 22). This indicates that additional reductions in coolant pressure drop beyond a conventionally cooled chamber are possible using HARCC before the hot-gas-

side wall temperature would reach that of a conventionally cooled chamber.

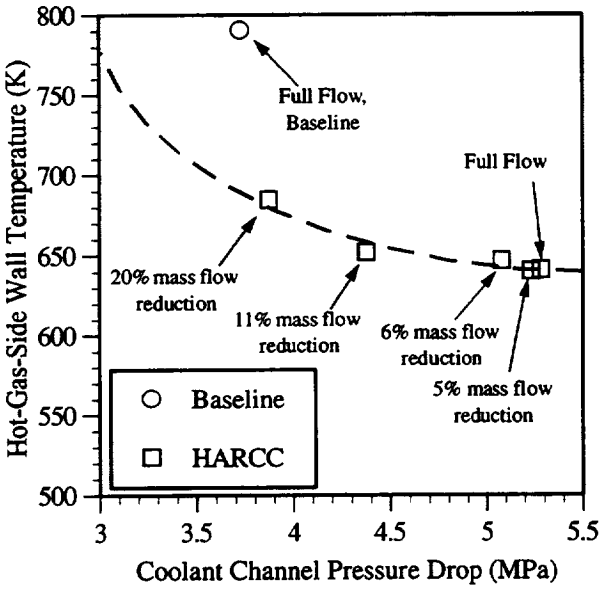

Figure 22. - Coolant pressure drop versus hot-gas-side wall temperature for reduced coolant mass flow rates at a nominal chamber pressure of 11 MPa (1600 psia).

Conclusions

The HARCC concept was successfully validated using an extensively instrumented, 89kN (20,000 lb_f) combustion chamber. The HARCC chamber sustained 29 thermal cycles with no visible damage to the throat area. Comparison of the instrumentation data with two analysis methods revealed that coupling of the codes RTE and TDK could predict the rib thermocouple temperatures within an average of 9 percent and the coolant channel pressure drops within an average of 25 percent. Using the RTE/TDK method to predict the hot-gas-side wall temperature, HARCC were shown, and validated, to produce reductions of up to 25 percent, in the throat region, over a conventionally cooled combustion chamber. This compares well with the previous subscale experiments, which showed a hot-gas-side wall temperature reduction of 28 percent. Additionally, HARCC were shown to accommodate reduced coolant mass flow rates and reduced coolant pressure drop while retaining at least a 13 percent decrease in the hot-gas-side wall temperature over that of a conventionally cooled combustion chamber. This validates the potential to decrease coolant pressure requirements from the turbomachinery by reductions in the coolant flow required to obtain the same cooling as a conventionally cooled rocket engine.

References

1. Carlile, J.A., Quentmeyer, R.J.: An Experimental Investigation of High-Aspect-Ratio Cooling Passages, 28th Joint Propulsion Conference, 1992, AIAA-92-3154 (Also NASA TM-105679).
2. Wadel, M.F., Quentmeyer, R.J., Meyer, M.L.: A Rocket Engine Design for Validating the High Aspect Ratio Cooling Channel Concept, NASA Conference Publication 3282, Vol. II, pp. 145-150.
3. Naraghi, M.H.N.:User's Manual, RTE - A Computer Code for Three-Dimensional Rocket Thermal Evaluation, Manhattan College, Riverdale, NY, September 1993, under NASA grant NAG 3-892.
4. Nickerson, G.R., Coats, D.E., Dang, A.L., Dunn, S.S., Kehtarnavaz, H.: Two-Dimensional Kinetics (TDK) Nozzle Performance Computer Program, NAS8-36863, March1989.
5. Muss, J.A., Nguyen, T.V., Johnson, C.W.: User's Manual for Rocket Combustor Interactive Design (ROCCID) and Analysis Computer Program, NASA Contractor Report 187109, Contract NAS3-25556, May 1991.

REPORT DOCUMENTATION PAGE

Form Approved
OMB No. 0704-0188

1. AGENCY USE ONLY (*Leave blank*)	2. REPORT DATE	3. REPORT TYPE AND DATES COVERED
	June 1996	Technical Memorandum

4. TITLE AND SUBTITLE

Validation of High Aspect Ratio Cooling in a 89 kN (20,000 lb_f) Thrust Combustion Chamber

5. FUNDING NUMBERS

WU-242-20-06

6. AUTHOR(S)

Mary F. Wadel and Michael L. Meyer

7. PERFORMING ORGANIZATION NAME(S) AND ADDRESS(ES)

National Aeronautics and Space Administration
Lewis Research Center
Cleveland, Ohio 44135-3191

8. PERFORMING ORGANIZATION REPORT NUMBER

E-10337

9. SPONSORING/MONITORING AGENCY NAME(S) AND ADDRESS(ES)

National Aeronautics and Space Administration
Washington, D.C. 20546-0001

10. SPONSORING/MONITORING AGENCY REPORT NUMBER

NASA TM-107270
AIAA-96-2584

11. SUPPLEMENTARY NOTES

Prepared for the 32nd Joint Propulsion Conference cosponsored by AIAA, ASME, SAE, and ASEE, Lake Buena Vista, Florida, July 1-3, 1996. Responsible person, Mary F. Wadel, organization code 5310, (216) 977-7510.

12a. DISTRIBUTION/AVAILABILITY STATEMENT

Unclassified - Unlimited
Subject Categories 20 and 34

This publication is available from the NASA Center for AeroSpace Information, (301) 621-0390.

12b. DISTRIBUTION CODE

13. ABSTRACT (*Maximum 200 words*)

In order to validate the benefits of high aspect ratio cooling channels in a large scale rocket combustion chamber, a high pressure, 89 kN (20,000 lb_f) thrust, contoured combustion chamber was tested in the NASA Lewis Research Center Rocket Engine Test Facility. The combustion chamber was tested at chamber pressures from 5.5 to 11.0 MPa (800-1600 psia). The propellants were gaseous hydrogen and liquid oxygen at a nominal mixture ratio of six, and liquid hydrogen was used as the coolant. The combustion chamber was extensively instrumented with 30 backside skin thermocouples, 9 coolant channel rib thermocouples, and 10 coolant channel pressure taps. A total of 29 thermal cycles, each with one second of steady state combustion, were completed on the chamber. For 25 thermal cycles, the coolant mass flow rate was equal to the fuel mass flow rate. During the remaining four thermal cycles, the coolant mass flow rate was progressively reduced by 5, 6, 11, and 20 percent. Computer analysis agreed with coolant channel rib thermocouples within an average of 9 percent and with coolant channel pressure drops within an average of 20 percent. Hot-gas-side wall temperatures of the chamber showed up to 25 percent reduction, in the throat region, over that of a conventionally cooled combustion chamber. Reducing coolant mass flow yielded a reduction of up to 27 percent of the coolant pressure drop from that of a full flow case, while still maintaining up to a 13 percent reduction in a hot-gas-side wall temperature from that of a conventionally cooled combustion chamber.

14. SUBJECT TERMS	15. NUMBER OF PAGES
Rocket combustors; Rocket engine cooling; Aspect ratio; Chamber liner	12
	16. PRICE CODE: A03

17. SECURITY CLASSIFICATION OF REPORT	18. SECURITY CLASSIFICATION OF THIS PAGE	19. SECURITY CLASSIFICATION OF ABSTRACT	20. LIMITATION OF ABSTRACT
Unclassified	Unclassified	Unclassified	

National Aeronautics and
Space Administration

Lewis Research Center
21000 Brookpark Rd.
Cleveland, OH 44135-3191